LITERATURE CITED

1. V. Z. Parton and P. I. Perlin, Methods of the Mathematical Theory of Elasticity [in Russian], Nauka, Moscow (1981).
2. H. Bateman and A. Erdelyi, Tables of Integral Transforms, McGraw-Hill, New York (1954).
3. A. T. De Hoop, "A modification of Cagniard's method for solving seismic pulse problems," Appl. Sci. Res., Ser. B, 8 (1960).
4. P. Bannerjee and R. Butterfield, Methods of Boundary Elements in Applied Sciences [Russian translation], Mir, Moscow (1984).
5. V. A. Babeshko, Generalized Method of Factorization in Three-Dimensional Dynamical Mixed Problems of Elasticity Theory [in Russian], Nauka, Moscow (1984).

CONJUGATE PROBLEM OF AERODYNAMIC EXTRUSION OF JETS OF HEATED VISCOUS LIQUID

V. I. Eliseev and L. A. Fleer

UDC 532.526

Aerodynamic extrusion of jets of viscous liquids is of practical value for the production of synthetic filaments consisting of polymer melts with the help of high-velocity gas flows. The problem of fiber formation is a conjugate problem, in which the mutual effect of the fiber formed and the surrounding medium must be taken into account. This problem was first formulated mathematically in [1, 2], where a model of the flow is proposed and the basic equations and boundary conditions are derived. In [3, 4] the most general equations describing the dynamics of thin jets of viscous liquid are derived taking into account the spatial bending and twisting, and in [4-6] the present status of the theory of hydrodynamics, heat transfer, and stability of fiber formation processes are analyzed in detail. In the case of fiber formation with the help of extrusion devices with low (up to 5 m/sec) final velocities of the jets, the external force exerted by the flow can be neglected [7]. As the velocity of the filament increases the effect of friction on the parameters of the fiber becomes significant. For aerodynamic extrusion the forces of interaction of the fiber and flow are determining. A number of works (for example, [8, 9]), in which the characteristics of aerodynamic formation are studied, are devoted to some physical and technological aspects of this problem. In this paper we construct a complete, conjugate mathematical model of the flow and we perform a numerical analysis based on an iteration method [10, 11].

1. Basic Equations and Boundary Conditions. Figure 1 shows a diagram of the flow of a jet of liquid, extruded with an air flow, parallel to the axis of the jet (1 – draw hole, 2 – jet, 3 – ejector). Because of the existence of viscous and heat-conduction effects, the jet of melt and the exterior medium interact with one another by means of the boundary layer. The mutual effect of the extruded jet and the medium makes this problem a conjugate problem. Let us assume that the flow of the jet of melt is stable, the jet does not bend and does not oscillate, and the velocity and temperature profiles in the jet are uniform. These assumptions make it possible to employ simple equations of motion of the liquid jet and heat transfer, derived, for example, in [1-3]:

$$\frac{dA_j}{dx} = \frac{\rho_j A_j}{G\beta} F, \quad \frac{dT_j}{dx} = \frac{2\pi r_j q}{\rho_j u_j c_j A_j},$$
$$G = \rho_j u_j A_j, \; F = F_{fr} + F_{in} + F_g, \; q = q_T + q_{rad} \qquad (1.1)$$
$$\beta = D \exp(B/T_j + C), \; A_j|_{x=0} = A_{j0}, \; T_j|_{x=0} = T_{j0}.$$

Here ρ_j is the density of the liquid; u_j is the velocity of the jet; ε is the emissivity of the body; σ is the Stefan–Boltzmann constant; c_j is the heat capacity of the liquid; A_j is the area of the transverse cross section of the jet; T_j is the temperature of the jet; β is the longitudinal viscosity of the polymer; G is the flow rate of the polymer; r_j is the radius of the jet; F is the total axial force, balancing the rheological force and including

Dnepropetrovsk. Translated from Zhurnal Prikladnoi Mekhaniki i Tekhnicheskoi Fiziki, No. 6, pp. 148-153, November-December, 1988. Original article submitted August 18, 1987.

0021-8944/88/2906-0903$12.50

the force of friction, the weight of the jet, and inertia $\left(F_{fr}=2\pi\int_x^L \tau_j r_j (1+r_{jx}'^2)^{0.5}dx,\quad F_g=\int_x^L g\rho_j A_j dx\right.$ and $\left.F_{in}=G(u_j-u_L)\right)$; L is the length of the jet; u_L is the final velocity of the jet; τ_j is the tangential stress on the surface of the jet; q_T is the heat flux owing to forced convection; $q_{rad}=\varepsilon\sigma(T_j^4-T_\infty^4)$ is the radiative heat flux; T_∞ is the temperature of the medium on the outer boundary of the boundary layer; and D, B, and C are parameters of a specific polymer. To close (1.1) the equations for the laminar boundary layer on a long, thin, body of revolution

$$u\frac{\partial u}{\partial x}+v\frac{\partial u}{\partial y}=\nu\left(\frac{\partial^2 u}{\partial y^2}+\frac{1}{y}\frac{\partial u}{\partial y}\right),$$
$$\frac{\partial(yu)}{\partial x}+\frac{\partial(yv)}{\partial y}=0,\quad \rho c_p\left(u\frac{\partial T}{\partial x}+v\frac{\partial T}{\partial y}\right)=\lambda\left(\frac{\partial^2 T}{\partial y^2}+\frac{1}{y}\frac{\partial T}{\partial y}\right) \tag{1.2}$$

and the boundary conditions

$$u|_{y=r_j}=u_j,\quad T|_{y=r_j}=T_j, \tag{1.3}$$
$$u|_{y=r_j+\delta_D}=u_\infty,\quad T|_{y=r_j+\delta_T}=T_\infty,\quad \tau_j=\mu\frac{\partial u}{\partial y}\Big|_{y=r_j},\quad q_T=-\lambda\frac{\partial T}{\partial y}\Big|_{y=r_j},$$

must be added. Here u and v are the velocity components of the gas; T is the temperature of the gas; ρ is the density; c_p is the heat capacity; λ is the coefficient of thermal conductivity; ν and μ are the kinematic and dynamic viscosities of the gas; u_∞ is the velocity of the exterior flow; δ_D, δ_T are the thickness of the dynamic and thermal boundary layers; and τ_j is the friction stress between the jet and the gas. Many constructional schemes for forming the jet are now known, but they can all be reduced to simple physical models, differing by the boundary conditions at infinity and the combination of regimes of flow around the jet of melt. In what follows we shall examine some formation schemes that are of theoretical and practical interest.

2. Laminar Flow around the Jet. In this case the flow scheme corresponds to Fig. 1 with $L_2 = 0$. We assume that u_∞, the thermophysical parameters of the gas, and T_∞ are constant. We shall solve the system (1.2) by the integral method, where logarithmic profiles, which have been successfully employed in problems of this type [11, 12], are employed as approximating functions for the velocity and temperature (2.1):

$$\frac{u}{u_j}=1+\frac{1}{\alpha}\ln\left(1+\frac{y}{r_j}\right),\quad \frac{T}{T_j}=1-\frac{1}{\xi}\ln\left(1+\frac{y}{r_j}\right). \tag{2.1}$$

Taking into account the boundary conditions (1.3) and the assumptions made, after Eqs. (1.2) are integrated over the transverse coordinate y for unknown forms of the parameters α and ξ we obtain

$$\frac{d\alpha}{dx}=\frac{\frac{2\nu\alpha^2}{u_j r_j^2}+2\frac{r_{jx}'}{r_j}\alpha\left(R_1-\frac{u_\infty}{u_j}R_2\right)}{R_3},$$
$$R_1=-\alpha^2\gamma-\frac{\alpha}{2}+\frac{\alpha\gamma}{2}+0.5+e^{2\alpha\gamma}\left(\frac{\alpha\gamma}{2}+\frac{\alpha}{2}-0.5\right),$$
$$R_2=\alpha^2+\frac{\alpha}{2}+e^{2\alpha\gamma}\left(\alpha^2\gamma+\alpha^2-\frac{\alpha}{2}\right),$$
$$R_3=\frac{\alpha}{2}-\frac{\alpha\gamma}{2}-1+e^{2\alpha\gamma}\left(-\frac{3}{2}\alpha\gamma-\frac{\alpha}{2}+1+\alpha^2\gamma^2+\alpha^2\gamma\right),$$
$$\frac{d\xi}{dx}=\left[-\frac{\nu}{\mathrm{Pr}}\frac{1}{u_j r_j^2\xi}+\frac{T_{jx}'}{T_\infty-T_j}\left(R_4+\frac{u_\infty}{u_j}R_5\right)-\frac{2r_{jx}'}{r_j}\frac{u_\infty}{u_j}R_5-\right.$$
$$\left.-\alpha_x'\left(R_6+\frac{u_\infty}{u_j}R_7\right)-\gamma_x'\left(R_8+\frac{u_\infty}{u_j}R_9\right)\right]\Big/\left(R_{10}+\frac{u_\infty}{u_j}R_{11}\right), \tag{2.2}$$

$$R_4=e^{2\alpha\gamma}\left(0.5+\frac{\gamma}{2}-\frac{1}{4\alpha}+\frac{\alpha\gamma}{2\xi}-\frac{1}{4\xi}+\frac{\alpha\gamma^2}{2\xi}-\frac{\gamma}{2\xi}+\frac{1}{4\alpha\xi}\right)-\frac{1}{2}+\frac{1}{4\alpha}+\frac{1}{4\xi}-\frac{1}{4\alpha\xi},$$

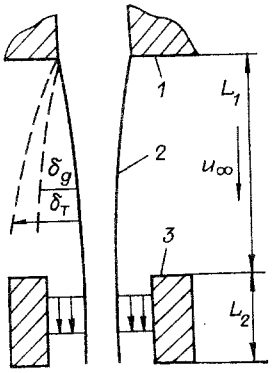

Fig. 1

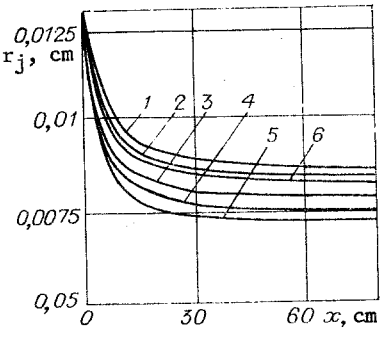

Fig. 2

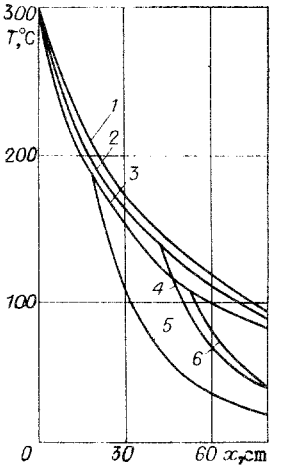

Fig. 3

$$R_5 = e^{2\alpha\gamma}\left(\frac{1}{4\xi} - \frac{\alpha\gamma}{2\xi} - \frac{1}{2}\right) - \frac{e^{-2\xi}}{4\xi},$$

$$R_6 = e^{2\alpha\gamma}\left(\gamma + \frac{\alpha\gamma^3}{\xi} + \gamma^2 - \frac{\gamma}{2\alpha} + \frac{\alpha\gamma^2}{\xi} - \frac{\gamma^2}{2\xi} + \frac{\gamma}{2\alpha\xi} + \frac{1}{4\alpha^2} - \frac{1}{4\alpha^2\xi}\right) + \frac{1}{4\alpha^2\xi} - \frac{1}{4\alpha^2},$$

$$R_7 = -\gamma e^{2\alpha\gamma}\left(\frac{\alpha\gamma}{\xi} + 1\right), \quad R_8 = e^{2\alpha\gamma}\left(\alpha + \frac{\alpha^2\gamma}{\xi} + \alpha\gamma + \frac{\alpha^2\gamma^2}{\xi}\right),$$

$$R_9 = -\alpha e^{2\alpha\gamma}\left(\frac{\alpha\gamma}{\xi} + 1\right),$$

$$R_{10} = e^{2\alpha\gamma}\left(-\frac{\alpha\gamma}{\xi^2} + \frac{1}{4\xi^2} - \frac{\alpha\gamma^2}{2\xi^2} + \frac{\gamma}{2\xi^2} - \frac{1}{4\alpha^2\xi^2}\right) + \frac{1}{4\alpha\xi^2} - \frac{1}{4\xi^2},$$

$$R_{11} = e^{2\alpha\gamma}\left(\frac{\alpha\gamma}{2\xi^2} - \frac{1}{4\xi^2}\right) + e^{-2\xi}\left(\frac{1}{4\xi^2} + \frac{1}{2\xi}\right), \quad \gamma = \frac{u_\infty}{u_j} - 1$$

(Pr is the Prandtl number of the gas).

Because Eqs. (2.2) have a singularity at the point x = 0, the initial conditions neglecting higher-order infinitesimals for $x \to 0$ assume the form

$$\alpha_0 = \left[\frac{4\nu x}{r_j^2 u_j\left(\frac{\gamma^3}{3} + \gamma^2\right)}\right]^{0.5}, \quad \xi_0 = \alpha_0\left[\frac{\frac{\gamma^2}{2} + \left(\frac{\gamma^4}{4} + \frac{\gamma^3}{2} + \frac{\gamma^2}{2}\right)^{0.5}}{\gamma + 1}\right]. \tag{2.3}$$

Thus the problem of aerodynamic formation in this formulation reduces to solving numerically the systems (1.1) and (2.2) with the appropriate boundary conditions. The iteration process was constructed based on how close the resulting longitudinal force at the end of the section of formation is to zero with a prefixed accuracy. The starting data corresponded to real regimes of formation of the polymer polyester teraphthalate (PETP): r_{j_0} = 0.0125 cm, T_{j_0} = 300°C, T_∞ = 17°C, G = 0.029 g/sec, the length of the section of formation L_1 = 80 cm, and the molecular weight of the polymer M = 25,000 specific units.

Figures 2 and 3 show the dependences $r_j(x)$ and $T_j(x)$, obtained for u_∞ = 3, 5, and 10 m/sec – the curves 1-3 (without the transition into the turbulent state). It follows from calculations that the extruding flow around the fiber cools the fiber quite rapidly, and in spite of the comparatively large difference between the velocities u_∞ the instantaneous temperatures of the jet are quite close (the difference between the curves 1 and 3 does not exceed 15%). Because the viscosity of the polymer grows rapidly as the temperature decreases the diameter of the filaments also quite rapidly reaches a constant value. As the rate of flow around the jet increases the final diameter of the jet decreases somewhat, but the zone of intense change in the diameter becomes shorter.

3. Mixed Regime of Flow past the Jet. Under real conditions the boundary layers on the filaments can be both laminar and turbulent, since the length of the formation zone can reach several tens of thousands with respect to the diameter of the draw hole. It is shown in [5, 13] that the turbulent regime of flow past the fiber corresponds to an instantaneous Reynolds number $\mathrm{Re}_x = x(u_\infty - u_j)/\nu$ of the order of 10^5, and heat transfer and the interaction force are described by a number of close criterional relations, presented in [1, 5, 12, 13]. In the present calculations we employed the criterional relations from [1, 13]:

$$\mathrm{Nu} = 0.42\mathrm{Re}^{0.334},\ C_f = 0.3745\mathrm{Re}^{-0.61},\ \mathrm{Re} = 2r_j(u_\infty - u_j)/\nu. \tag{3.1}$$

At the present time there is no sufficiently accurate theory of turbulent and transitional layers on thin axisymmetric bodies, so that to make the estimates we shall assume that the laminar flow around the jet exists until Re_x reaches a critical value, after which a fully developed, turbulent, boundary layer starts.

In this case the calculation is first performed based on Eqs. (1.1) and (2.2), and then based on (1.1) and (3.1). Figures 2 and 3 show the distribution of the values r_j and T_j along the length of the formation section for the following regimes: the coordinate of the point of transition $x_* = 42$ cm corresponds to the critical value $\mathrm{Re}_x = 10^5$ and velocity u_∞ = 5 m/sec (curve 4); u_∞ = 10 m/sec corresponds to $x_* = 17$ cm (curve 5); $\mathrm{Re}_x = 3\cdot10^5$ and u_∞ = 10 m/sec corresponds to $x_* = 53$ cm (curve 6). One can see from Figs. 2 and 3 that the introduction of the relations for a turbulent boundary layer into the computational scheme has a strong effect on the instantaneous temperature of the jet and to a lesser extent on its radius; this is attributable to the viscosity of the cooled jet.

4. Extrusion with the Help of an Ejector. In this case the jet of melt is extruded from the draw hole by means of a turbulent flow of gas, moving in the ejector (see Fig. 1). It was assumed that up to the ejector the jet moves in a stationary gas and a laminar boundary layer develops on it. The calculation up to the zone of the ejector with a given extrusion force is a particular case of the problem posed here; it is performed in a number of works (see, e.g., [10]). For ejector extrusion the calculation in the formation zone is performed based on (1.1) and (2.2) for $u_\infty = 0$, and in the ejector zone based on (1.1) and (3.1) with a given velocity of the turbulent flow that is constant over the cross section and length of the ejector. In the equation of balance of forces from (1.1) in the ejector zone the term F_{extr} – the extrusion force – generated by the ejector is added to the terms: $F = F_{extr} + F_{fr} + F_{in} + F_g$.

The distance from the draw hole to the ejector L_1, the length of the ejector L_2, and the velocity of the gas in the ejector correspond to the parameters of a real construction for fiber formation. Figures 4 and 5 show the functions $r_j(x)$ and $T_j(x)$ with L_1 = 60 cm and L_2 = 20 cm; the velocity of the gas in the ejector $u_{\infty ej}$ = 10, 50, and 100 m/sec (curves 1-3). As follows from the calculations, the extrusion process is completed in the section L_1; this is linked with the strong cooling of the jet of melt in the ejector for all velocities of the ejecting gas presented (Fig. 4, curves 1-3), and the distribution of the instantaneous radius of the jet along its length depends strongly on the velocity of the gas in the ejector (Fig. 5, curves 1-3). Figure 4 shows the distribution of the absolute values of the components of the force balance along the length of the jet for $u_{\infty ej}$ = 100 m/sec. The maximum value of the rheological force on the inlet into the ejector corresponds to the extrusion force of the ejector. The greatest resistance to extrusion in the pre-ejector zone ($x < 60$ cm) is exerted by the force of inertia (~55% of the pulling force), since the jet accelerates from ~0.5 up to ~20 m/sec. The aerodynamic resistance is about 11%. The contribution of the force of gravity to the pulling force is small (less than 5%). In the ejector zone (60 cm < x < 80 cm) the chief acting force is the force of friction. Since the

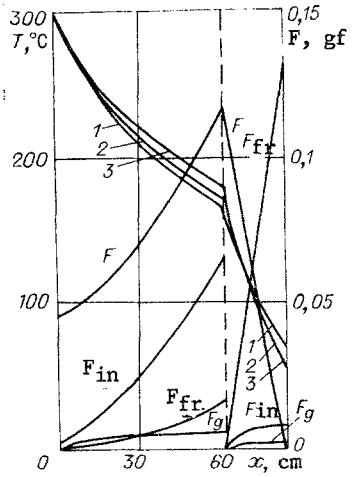

Fig. 4

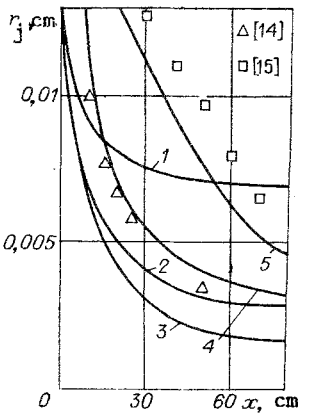

Fig. 5

flow of heat from the jet into the ejector is strong, the acceleration of the jet is low owing to the high viscosity and the force of inertia equals ~6% of the force of friction, whereas the contribution of the weight of the jet to the extrusion force is insignificant (less than 1%).

In the general case the gas jet emanating from the ejector creates an additional pulling force, which is not taken into account in the model problem described, since the post-ejector zone does not contribute anything fundamentally new to the computational scheme under study, but under real conditions the fiber immediately beyond the post-ejector zone is diverted into the receiving unit without an increase in the velocity. Experiments on formation from a melt with the help of a ring-shaped nozzle ejecting the jet were performed in [8, 9], but because their description is incomplete the results of [14, 15] on the fiber formation with a gas at rest for a fixed velocity of the jet were employed to evaluate the results obtained. Comparison of the computational results with the experimental results indicates that the flow model and the solution method presented in this paper are correct. Curve 4 in Fig. 5 shows the instantaneous radius of the jet of PETP melt for conditions of formation of [14], while curve 5 corresponds to the conditions of formation in [15]. The maximum discrepancy between the computational data and the experimental data does not exceed 20%.

LITERATURE CITED

1. S. Kase and T. Matsuo, "Studies on melt spinning. 1. Fundamental equations on the dynamics of melt spinning," J. Polym. Sci. A, 3, No. 7 (1965).
2. T. Matsuo, H. Yasuda, and H. Sugiyama, "Phenomenological theories for melt spinning process and their applications," Proceedings of the 2nd International Symposium on the Chemistry of Fibers, Kalinin (1977), Vol. 2.
3. V. M. Entov and A. L. Yarin, "Dynamics of jets of a droplet liquid," Preprint No. 127, Institute of Applied Mechanics, Academy of Sciences of the USSR, Moscow (1979).
4. V. M. Entov and A. L. Yarin, "Dynamics of free jets and films of viscous and rheological complex liquids," in: Progress in Science and Technology, VINITI. MZhG (1984), Vol. 18.
5. A. Zyabitskii, Theoretical Foundations of the Formation of Chemical Fibers [in Russian], Khimiya, Moscow (1979).
6. Chang Dei Kahn, Rheology in Polymer Processing [in Russian], Khimiya, Moscow (1979).
7. D. V. S. Kherla (ed.), Structure of Fiber [in Russian], Khimiya, Moscow (1968).
8. A. V. Genis, D. V. Fil'bert, and A. A. Sindeev, "Balance of forces in aerodynamic formation of filaments from polypropylene melt," Khim. Volokna, No. 3 (1978).
9. A. V. Genis, D. V. Fil'bert, and A. A. Sindeev, "Aerodynamic formation of a fiber from a melt," Khim. Volokna, No. 1 (1978).
10. V. I. Eliseev, L. A. Fleer, and B. P. Belozerov, "Direct and inverse conjugate problems of the theory of formation of synthetic fibers," in: Heat and Mass Transfer VII, Institute of Heat and Mass Transfer, Minsk (1984), Vol. 5, Part 2.
11. D. E. Bourne and D. G. Elliston, "Heat transfer through the axially symmetric boundary layer on a moving circular fibre," Int. J. Heat Mass Transfer, 13, No. 3 (1976).
12. V. R. Borovskii and V. A. Shelimanov, Heat Exchange of Cylindrical Bodies with Small Radii and their Systems [in Russian], Naukova Dumka, Kiev (1985).

13. M. Matsui, "Air drag on a continuous filament in melt spinning," Trans. Soc. Rheol., 20, No. 3 (1976).
14. G. Wilhelm, "Die Abkühlung eines aus der Schmelze gesponnenen polymeren Faden im Spinnschucht," Kolloid-Zeitschrift., 208, No. 2 (1966).
15. P. Köhler, "Berührungslose Bestimmung von Temperaturen und Durchmessern an einem aus der Schmelze gesponnenen Faden," Chemi-Ing. Techn., 43, No. 5 (1971).

NUMERICAL MODELING OF PHYSICAL EFFECTS IN THE DRAWING OF A GLASSY MATERIAL INTO A FIBER

E. M. Dianov, S. M. Perminov, V. N. Perminova, and V. K. Sysoev

UDC 532.6.011.72

This article is devoted to the numerical modeling of the physical effects which take place in the conversion of a glassy substance from a semifinished product into a fiber by drawing while it is in the hot, viscoplastic state. The problem being examined relates to a number of so-called "problems with a free boundary," since the surface of the highly viscous molten material, not in contact with any other surface, changes form in accordance with the laws governing the dynamic equilibrium between gravitation, surface tension, and other forces. A characteristic feature of the problem is the presence of large gradients of temperature, viscosity, and fluid velocity in the drawing zone. We studied the effect of stable drawing of the semifinished product into a fiber, as well as the conditions, character, and causes of underheating or overheating. The effects of drop formation and fiber rupture are also examined. The problem being considered is of great practical interest, since it helps answer a key question in one of the most rapidly developing high-precision technologies – the stability of the drawing of optical fibers from quartz glass [1-4].

The drawing of quartz glass was studied as the axisymmetric vertical flow of a highly viscous fluid with a free boundary and variable viscosity. Viscosity unambiguously depends on the temperature of the quartz glass [5] in the drawing zone and changes from 10^4 to 10^{20} P. The conditions of entry of heat into the semifinished product are assumed to be given.

We will study coupled nonlinear nonsteady equations describing the heat transfer and flow of a viscous incompressible liquid and its free boundary, along with the continuity equations [2, 4, 6]:

$$\frac{\partial T}{\partial t}+u\frac{\partial T}{\partial r}+v\frac{\partial T}{\partial z}=-\frac{1}{\rho C_p}\left(\frac{\partial}{\partial r}+\frac{\partial}{\partial z}\right)k(T)\left(\frac{\partial}{\partial r}+\frac{\partial}{\partial z}\right)T+\frac{1}{\rho C_p}k(T)\left[\frac{\partial^2}{\partial r^2}+\frac{1}{r}\frac{\partial}{\partial r}+\frac{\partial^2}{\partial z^2}\right]T; \tag{1}$$

$$\frac{\partial u}{\partial t}+u\frac{\partial u}{\partial r}+v\frac{\partial u}{\partial z}=-\frac{1}{\rho}\frac{\partial p}{\partial r}+\eta(T)\left[\frac{\partial^2 u}{\partial r^2}+\frac{\partial^2 u}{\partial z^2}+\frac{1}{r}\frac{\partial u}{\partial r}-\frac{u}{r^2}\right]+2\frac{\partial u}{\partial r}\frac{\partial \eta(T)}{\partial r}+\frac{\partial \eta(T)}{\partial z}\left(\frac{\partial v}{\partial r}+\frac{\partial u}{\partial z}\right),$$

$$\frac{\partial v}{\partial t}+u\frac{\partial v}{\partial r}+v\frac{\partial v}{\partial z}=-\frac{1}{\rho}\frac{\partial p}{\partial z}+\eta(T)\left[\frac{\partial^2 v}{\partial r^2}+\frac{\partial^2 v}{\partial z^2}+\frac{1}{r}\frac{\partial v}{\partial r}\right]+g+2\frac{\partial v}{\partial z}\frac{\partial \eta(T)}{\partial z}+\frac{\partial \eta(T)}{\partial r}\left(\frac{\partial v}{\partial r}+\frac{\partial u}{\partial z}\right); \tag{2}$$

$$\frac{\partial u}{\partial r}+\frac{\partial v}{\partial z}+\frac{u}{r}=0; \tag{3}$$

$$\frac{\partial a}{\partial t}=-v\frac{\partial a}{\partial z}+u. \tag{4}$$

Here, the z axis is directed along the drawing axis; the r axis is perpendicular to the drawing axis; v and u are the longitudinal and transverse velocities of the molten quartz

Moscow. Translated from Zhurnal Prikladnoi Mekhaniki i Tekhnicheskoi Fiziki, No. 6, pp. 153-156, November-December, 1988. Original article submitted February 27, 1987.

 0021-8944/88/2906-0908$12.50